IEEE Access
Multidisciplinary | Rapid Review | Open Access Journal

Received April 28, 2018, accepted June 1, 2018, date of publication June 7, 2018, date of current version June 26, 2018.

Digital Object Identifier 10.1109/ACCESS.2018.2844802

Low-Velocity Impact Localization on Composites Under Sensor Damage by Interpolation Reference Database and Fuzzy Evidence Theory

HONGYANG LI[1], ZHONGYU WANG[1], JEFFREY YI-LIN FORREST[2,3], AND WENSONG JIANG[1], (Member, IEEE)

[1]School of Instrument Science & Opto-electronics Engineering, Beihang University, Beijing 100191, China
[2]Department of Mathematics, Slippery Rock University, Slippery Rock, PA 16057, USA
[3]School of Business, Slippery Rock University, Slippery Rock, PA 16057, USA

Corresponding author: Zhongyu Wang (mewan@buaa.edu.cn)

This work was supported in part by the Technological Foundation of China under Grant J132012c001 and in part by the Natural Science Foundation of China under Grant 51575032.

ABSTRACT Composites are widely used in aeronautical manufacturing. Despite their excellent properties, composites suffer from barely visible impact damage caused by low-velocity objects. Random impacts need to be detected and located to alert pilots and engineers of the need for maintenance. Generally, fiber Bragg grating (FBG) sensors are installed in aerospace composites, and a reference database is established by recording the reference signals from different impact positions. The random impact is located by comparing its signal to the reference signals in the database. The performance of current localization algorithms mainly relies on the repeatability of FBG signals. However, the FBG sensors or their installation structures may be damaged by repeated impacts during the monitoring process, and the localization accuracy will decrease. In this paper, a new algorithm is proposed based on the interpolation reference database and fuzzy evidence theory to realize accurate impact localization under sensor damage. More correlation coefficients are obtained from the basic reference database by interpolation, and the influence of damaged sensors on localization results is reduced by fuzzy evidence theory. The proposed algorithm was tested on a carbon fiber reinforced polymer plate with four surface-attached FBG sensors. A parametric study was conducted to determine the coefficients of the algorithm. The localization performance was analyzed with both properly functioning sensors and damaged sensors. The results showed that the localization accuracy was better than the existing algorithms, especially in the case of sensor damage.

INDEX TERMS Low-velocity impact localization, fiber Bragg grating (FBG), sensor damage, interpolation reference database, fuzzy evidence theory.

I. INTRODUCTION

Composites are increasingly replacing conventional isotropic materials for aerospace applications because of their higher specific stiffness and strength [1]. Specifically, carbon fiber reinforced polymer (CFRP) plates have been widely used in the manufacture of aircrafts. The CFRP plates are made of a number of carbon-fiber fabrics impregnated with polymer. The fabrics are stacked together with specified orientations and formed in high temperature and pressure. Meanwhile, the wide range of applications of composites has raised concern. Due to the lack of through-thickness reinforcement, the transverse damage resistance of composites is weak [2], [3]. The damage mechanism of composites is much more complex than that of conventional isotropic materials [4], [5]. Low- velocity impacts, caused by runway debris, bird strikes, tool drop, and ground vehicles hitting aircrafts, can lead to barely visible impact damage (BVID) of the composites. BVID is hard to detect by visual inspection, and it may grow over time without being discovered in a timely manner, ultimately leading to structural failure [6], [7].

There is an increasing demand for designing localization algorithms to detect and locate low-velocity impacts [8]. With the help of an automated warning system, the localization algorithms can alert pilots and engineers to inspect and maintain the specific impact position, which is significant for reducing the risk of structural failures [9], [10].

The commonly applied localization algorithms are neural network algorithms [11]–[14], wave propagation algorithms [15]–[17] and reference database algorithms. The reference database algorithms have motivated many scholars' interest because the algorithms could provide acceptable localization accuracy with a relatively small number of sensors [18]–[20]. Traditional reference database algorithms contain three basic steps. First, a certain number of training points are picked from the monitored region. The reference database is established by recording the reference signals of all the picked training points. Then, a random impact that needs to be located takes place. The algorithm calculates the correlation between the random impact signal recorded by one of the sensors and all the reference signals in its database to evaluate their similarities. The training point with the maximum correlation coefficient can be found according to the sensor. Finally, the mean value of the positions obtained by all the sensors is determined as the impact localization result of the algorithm.

Fiber Bragg grating (FBG) sensors, a type of fiber optic sensor, have been recognized as ideal choices for composite material impact localization applications [21]. A FBG sensor is made by inscribing grating in an optical fiber. The refractive index of the grating experiences a periodic modulation, which makes the fiber act as a band-pass filter. When a broadband light is injected into the fiber, the grating reflects one specific wavelength, named the Bragg wavelength. The Bragg wavelength is determined by the Bragg condition:

$$\lambda_B = 2n_{eff}\Lambda, \tag{1}$$

where n_{eff} is the effective refractive index of the fiber core, and Λ is the grating period. FBG sensors have many advantages such as low weight, small size, multiplexing capability and immunity to electromagnetic interference [22], [23]. Generally, FBG sensors are installed on composites. The vibration caused by impacts is transferred to the optical fibers through the installation structure, which can lead to the wavelength shift of FBG sensors. Several studies have demonstrated the application of FBG sensors for different low velocity impact localization algorithms. Park *et al.* [14] used the neural network algorithm to detect impact positions in a composite panel. A series of impact tests were performed on the designated points. The signals were captured by FBG sensors to train the neural network. The positions for unknown impact events were obtained using the recorded FBG signals and the trained neural network. Kirkby *et al.* [24] took into account the velocity variation of Lamb wave propagation with directions of composite material and located the impact according to the time of the wave arriving at FBG sensors. Rezayat *et al.* [25] measured vibration data of composite structures with FBG sensors. Then, the impact forces were localized and reconstructed according to inverse methods. In particular, the FBG sensors were widely used in reference database algorithms. Jang *et al.* [19] presented the feasibility of using FBG sensor to locate the impact in a CFRP plate based on the reference database algorithm. He established a database composed of premeasured reference impact signals at training points. Impact positions were determined by calculating the mean-squared value between the random impact signal and the reference signals. Shrestha *et al.* [20] investigated the impact localization results obtained with different FBG sensor arrays and demonstrated that the reference database algorithm can localize random impact points on a composite wing with both one-dimensional and two-dimensional array sensors. Kim *et al.* [26] introduced the normalized cross-correlation into the reference database algorithm. The localization errors were dramatically reduced owing to the improved method.

The localization accuracy of current algorithms mainly relies on the repeatability of a random impact signal and reference signals in the database. It is usually assumed that the sensing property of FBG sensors would not change over time. In fact, the FBG sensors or their installation structures can be damaged as they suffer from repeated impacts during the monitoring process. Fiber cladding can be broken by impacts, and therefore some light leaks out of the fiber, which leads to the variation in reflectance spectrum of FBG sensors. Besides, the installation structure may crack, and that changes the propagation characteristic of the vibration waves in the structure. The degree of damage will increase over time, which will change the sensing property of the FBG sensors. As a result, the random impact signal will differ from the reference signal at the same positions, and the localization accuracy will decrease. Moreover, the reference database algorithm determines the random impact position according to the training point with the maximum correlation coefficient. As the points are isolated, the localization accuracy of the algorithms is limited by the interval of the training points. Therefore, a versatile strategy to realize accurate localizations under sensor damage is needed to improve the accuracy and robustness of such impact localization systems. Fuzzy evidence theory is a hybrid theory combining the fuzzy sets with the evidence theory. The fuzzy sets are good at describing the uncertainty information caused by incomplete or imprecise measurements [27], [28], and the evidence theory is able to handle the conflicting data during evidence reasoning [29], [30]. The hybrid theory provides an opportunity to deal with instrument failure in engineering practices.

In this paper, a low-velocity impact localization algorithm based on interpolation reference database and fuzzy evidence theory is proposed. The interpolation reference database obtained more correlation coefficients based on the basic database by the double cubic polynomial interpolation. The intervals of the reference points are decreased to improve the localization accuracy. Moreover, the reliability of FBG sensors is assessed by the fuzzy sets. The influence of damaged sensors on the localization results is reduced based on evidence theory to enhance the robustness of the algorithm. The content of this paper is organized into five sections. Details of the proposed algorithm are described in Section 2. In Section 3, the experimental setup is outlined. A parametric

study is conducted to achieve the optimum performance of the proposed algorithms. In Section 4, the experimental results are discussed. The localization performance of the proposed algorithm is compared with the performance of other algorithms. Finally, conclusions are summarized in Section 5.

II. IMPACT LOCALIZATION ALGORITHM

The proposed impact localization algorithm consists of two main processes as shown in Fig. 1. First, the basic reference database is established by storing reference vectors S_{ref}. Once a random impact takes place, its vector S_{rand} is compared with reference vectors S_{ref} to calculate correlation coefficients R. The discrete R points are interpolated by the double cubic polynomial. Then, three fuzzy sets F_s, F_u, and F_{ud} are established, and all the positions are assessed based on their fuzzy set membership assignments $B_i(F_s)$, $B_i(F_u)$, and $B_i(F_{ud})$. The reliability of the FBG sensors is evaluated and data from different FBG sensors are fused to generate the integrated membership assignments $M(F_s)$, $M(F_u)$, and $M(F_{ud})$. The impact is located according to the evidence theory.

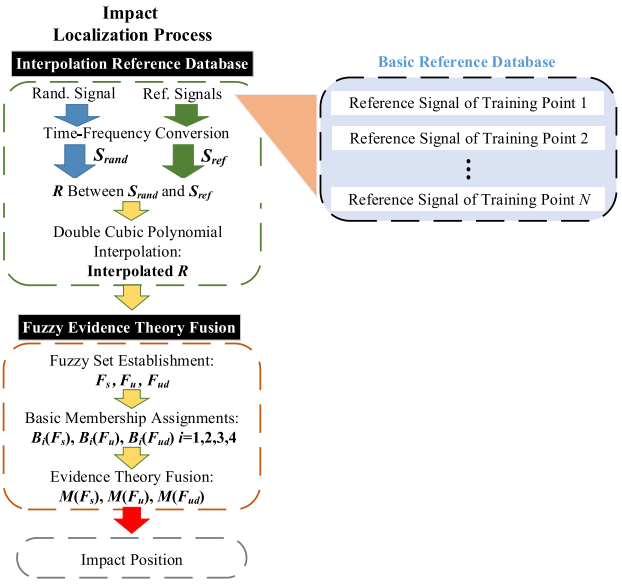

FIGURE 1. Process of Impact localization algorithm.

A. INTERPOLATION REFERENCE DATABASE

The reference database is established according to the array configuration of the FBG sensors. The most commonly used configuration is a rectangle-shaped monitored region with four FBG sensors at the corners of the rectangle as shown in Fig. 2. The sensors are attached in the direction of 45° to provide sufficient sensitivity. Training points are evenly distributed in the monitored region. The reference signals are generated by impacting the training points. The FBG sensors record the reference signals. The initial wavelengths are subtracted from the reference signals to eliminate the constant component, then signals are converted from the time domain to the frequency domain by Fourier

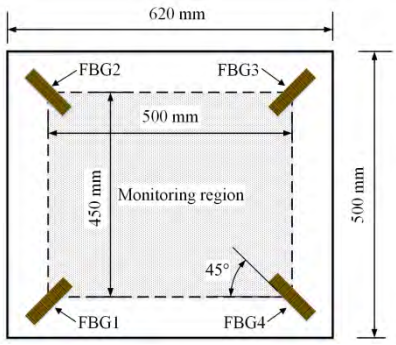

FIGURE 2. The configuration of the rectangle-shaped monitored region.

transformation. The frequency spectrum vectors of the reference signals are stored in the reference database as S_{ref}.

Different from reference signals, the signals caused by random impacts to be located are random impact signals. Once a random impact occurs, the signal is converted to the frequency spectrum vectors, which are defined as S_{rand}. To compare the similarity between S_{rand} and S_{ref}, the correlation coefficient R is calculated according to:

$$R = \frac{S_{ref} \cdot S_{rand}}{|S_{ref}||S_{rand}|}. \tag{2}$$

$|S_{ref}|$ and $|S_{rand}|$ are the 2-norms of S_{ref} and S_{rand}. R ranges from -1 to 1. If the random impact signal is similar to the reference signal, R tends to be 1. A set of R values is generated in a 2-dimensional plane by repeating the computing process with all of the reference signals as shown in Fig. 3(a). Values can be interpolated between the correlation coefficients at the training points. Thus, more reference points are obtained by the interpolation between the training points. As a short running time is important for the localization algorithm, the double cubic polynomial interpolation is used to balance the accuracy and the running time.

The double cubic polynomial interpolation uses cubic polynomials to fit the discrete points along both the x-axis and the y-axis of a 2-dimensional plane. In a monitored region with $m \times n$ training points, the point at the i-th row and the j-th column can be represented by (x_i, y_j). $R(x_i, y_j)$ is the R value at the point (x_i, y_j). First, the interpolation is along each row of the training points. The interpolation function is established as:

$$F_i(x) = a_i + b_i(x - x_i) + c_i(x - x_i)^2 + d_i(x - x_i)^3 \quad i = 1, \cdots, n-1, \tag{3}$$

where a_i, b_i, c_i, and d_i are the coefficient of the i-th interpolation piece. There are $n-1$ interpolation pieces for each row. The interpolation function along each row of training points can be determined [31]. In this way, m rows of interpolation functions can be obtained as shown in Fig. 3(b). Then, interpolation along each column is conducted. p columns of points are evenly inserted into every two adjacent columns. The R values of inserted points are calculated by substituting the coordinates into the corresponding interpolation

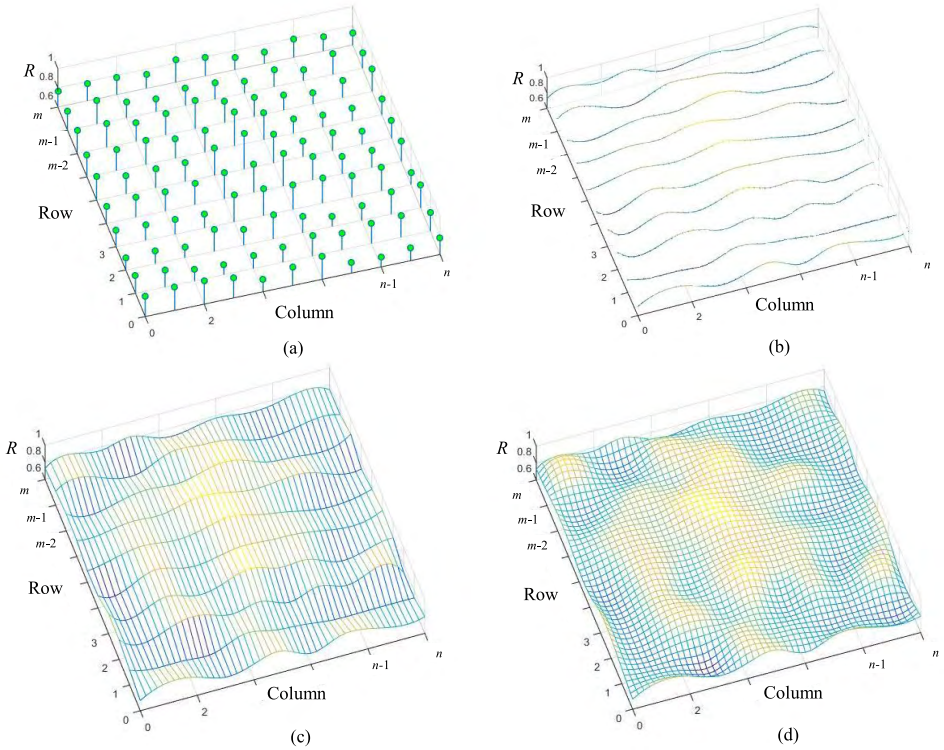

FIGURE 3. The process of double cubic polynomial interpolation. (a) Discrete R values in a 2-dimensional plane. (b) Interpolation along m rows of training points. (c) Interpolation along $(np - p + n)$ columns of reference points. (d) Interpolation along $(mq\text{-}q)$ rows of training points.

function $F_i(x)$. Hence, $(np - p + n)$ columns of interpolation functions can be obtained as shown in Fig. 3(c). Last, interpolation between adjacent rows is carried out. q rows of points are evenly inserted into every two adjacent rows, and q interpolation functions are determined according to R at the interpolating points. Hence, a total of $(mq - q)$ rows of interpolation functions can be obtained. Considering the $m$rows of interpolation functions in the first step, the number of reference points increases from $m \times n$ to $(np - p + n) \times (mq - q + m)$, where p and q are interpolation coefficients. The interpolation result is shown in Fig. 3(d).

B. FUZZY EVIDENCE THEORY FUSION

Each FBG sensor obtains a position with the maximum R according to the interpolation reference database. Current algorithms regard the mean value of the position coordinates obtained with four sensors as the final localization result. However, the sensors or their installation structures can be damaged by repeated impacts during the monitoring process, which leads to localization error. Since traditional impact localization algorithms cannot assess the measurement reliability of sensors, the localization error is brought to the final result, significantly reducing the localization accuracy.

Fuzzy evidence theory is introduced to fuse the data from the four sensors. Combining the fuzzy set and the evidence theory, the hybrid theory could make the correct judgment based on interference information. First, the fuzzy set is used to assess the reliability of the impact signals from FBG sensors. Three fuzzy sets are established. Shocked set F_s and non-shocked set F_u are used to indicate whether the impact belongs to this point. An undetermined set F_{ud} is used to describe the inconclusive impact signals. The measurement uncertainty caused by the sensor damage is taken into account by introducing the undetermined set. The belief degrees of the three fuzzy sets are described by basic membership assignments $B(F_s)$, $B(F_u)$, and $B(F_{ud})$, which are calculated based on the values of R as follows:

$$\begin{cases} B(F_s) = (1 + e^{\tau_1(R-c_1)})^{-1} \\ B(F_u) = e^{\frac{-(R-u)^2}{2\sigma^2}} \\ B(F_{ud}) = (1 + e^{\tau_2(R-c_2)})^{-1}, \end{cases} \tag{4}$$

where parameters u, and σ are the mean value and standard deviation of F_u; c_1 and c_2 are equal to the R values when $B(F_s) = 0.5$ and $B(F_{ud}) = 0.5$ respectively, which determine the boundary of the fuzzy set F_s and F_{ud}. τ_1 and τ_2 indicate the uncertainty of F_s and F_{ud} by influencing their gradients. There are $(np-p+n)\times(mq-q+m)$ reference points after the interpolation according to Section II. A. $C^2_{(np-p+n)\times(mq-q+m)}$ R values can be calculated based on statistical theory. The maximum, minimum, and average are $R_{\max}$, $R_{\min}$, and R_{aver}, respectively. The standard deviation is R_{sd}. The parameters

TABLE 1. Mechanical properties of the CFRP pre-preg.

Elasticity modulus E_{11} (GPa)	Elasticity modulus E_{22} (GPa)	Poisson's coefficient v_{13}	Poisson's coefficient v_{12}	Poisson's coefficient v_{23}	Shear modulus G_{12} (GPa)	Shear modulus G_{23} (GPa)
125	7	0.3	0.016	0.39	3.2	2.52

should satisfy:

$$\begin{cases} u = R_{\text{aver}} \\ \sigma = R_{\text{sd}} \\ c_1 = R_{\max} \\ c_2 = R_{\min} \\ (1 + e^{-\tau_1(1-c_1)})^{-1} > 0.999 \\ (1 + e^{\tau_2(0-c_2)})^{-1} > 0.999. \end{cases} \tag{5}$$

The basic memberships are normalized according to:

$$\begin{cases} m(F_s) \\ \quad = \dfrac{(1 + e^{-\tau_1(R-c_1)})^{-1}}{(1+e^{-\tau_1(R-c_1)})^{-1} + e^{\frac{-(R-u)^2}{2\sigma^2}} + (1+e^{\tau_2(R-c_2)})^{-1}} \\ m(F_u) \\ \quad = \dfrac{e^{\frac{-(R-u)^2}{2\sigma^2}}}{(1+e^{-\tau_1(R-c_1)})^{-1} + e^{\frac{-(R-u)^2}{2\sigma^2}} + (1 + e^{\tau_2(R-c_2)})^{-1}} \\ m(F_{ud}) \\ \quad = \dfrac{(1 + e^{\tau_2(R-c_2)})^{-1}}{(1+e^{-\tau_1(R-c_1)})^{-1} + e^{\frac{-(R-u)^2}{2\sigma^2}} + (1 + e^{\tau_2(R-c_2)})^{-1}} \end{cases} \tag{6}$$

As different memberships can be obtained with different sensors for certain random impact positions, evidence theory is introduced to address the data conflict [32]. The normalized memberships determined with four FBG sensors are combined to generate the integrated membership $M(F)$ as:

$$\begin{cases} M(F) = \dfrac{\sum_{F1 \cap F2 \cap F3 \cap F4 = F} m_1(F_1) m_2(F_2) m_3(F_3) m_4(F_4)}{1 - K} \\ \qquad\qquad for\ F \neq \emptyset \\ K = \sum_{F1 \cap F2 \cap F3 \cap F4 = \emptyset} m_1(F_1) m_2(F_2) m_3(F_3) m_4(F_4), \end{cases} \tag{7}$$

where F_1, F_2, F_3, and F_4 represent the fuzzy sets for FBG sensor 1 to FBG sensor 4; F_1, F_2, F_3, and F_4 can be F_s, F_u, or F_{ud}. F is the result of the intersection operation according to:

$$\begin{cases} F_s \cap F_s = F_s \\ F_u \cap F_u = F_u \\ F_{ud} \cap F_{ud} = F_{ud} \\ F_s \cap F_{ud} = F_s \\ F_u \cap F_{ud} = F_u \\ F_s \cap F_u = \emptyset \end{cases} \tag{8}$$

$m_1(F_1)$, $m_2(F_2)$, $m_3(F_3)$, and $m_4(F_4)$ are the memberships of F_1 to F_4. K represents the total conflict between the results of the 4 sensors. If a sensor is damaged, the random impact signal will be significantly different from its reference signals. R decreases and therefore the membership for F_{ud} is higher. The results of other undamaged sensors are adopted more according to (7) and (8). Hence, the influence of the damaged sensor on localization results is reduced.

The fusion process is conducted for all the reference points in the monitored region. Finally, the position with maximal shocked set membership is identified as the impact localization result. The data fusion process is shown in Fig. 4.

III. EXPERIMENTAL SETUP AND PROCEDURE

A. MATERIALS AND METHODS

The experiments were conducted on a 620 mm×500 mm CFRP plate. The plate was made of pre-impregnated unidirectional laminates. The elasticity modulus, Poisson's coefficients, and shear modulus of the material are shown in Table 1. The stacking process adopted for the plate was $[45/0/-45/90]_{4S}$. The numbers in the square bracket indicate the stacking sequence and directions (angles in degree) of the carbon-fiber fabrics in CFRP plate, and the subscript 4 means the stacking process defined in the bracket should be repeated four times and the s indicates symmetric arrangement. The total thickness of the plate is 4.6 mm.

An aluminum frame fully fixes the edges of the plate. Four FBG sensors with a grating length of 10 mm were used to detect the impact signals. The center wavelengths of these sensors are 1540, 1544, 1549, and 1554 nm, respectively. The sensors were attached to the undersurface of the composite plate. A commercial high-speed FBG demodulator Smart-Scan (Smart Fibres Ltd, United Kingdom) was used to demodulate the FBG sensor signals with 25 kHz sampling frequency. Low velocity impact was stimulated by an impact hammer, which is a spring-loaded mechanism. The hammerhead radius is 22 mm. The impact energy is adjustable with an accuracy of 0.1 J, and the maximum impact energy is 2J. The data processing was run on an Intel(R) core(TM) i7-4510U CPU at 2.6 GHz with 16 GB of RAM memory. The experimental apparatuses are shown in Fig. 5(a).

First, the training processes were conducted with properly functioning sensors. The training points have 50 mm space between two adjacent ones on the 500 mm×450 mm monitored region. Hence, there are 110 training points numbered from 1 to 110. The reference database was established according to Section II. A. Then, divide the monitored region equally into four quadrants named as local region 1 to 4. Five random impact points represented by target coordinates were chosen randomly on each region as illustrated in Fig. 5(b). Table 2 shows the coordinates of the 20 random impact points. The central axis of the hammer was vertically aimed

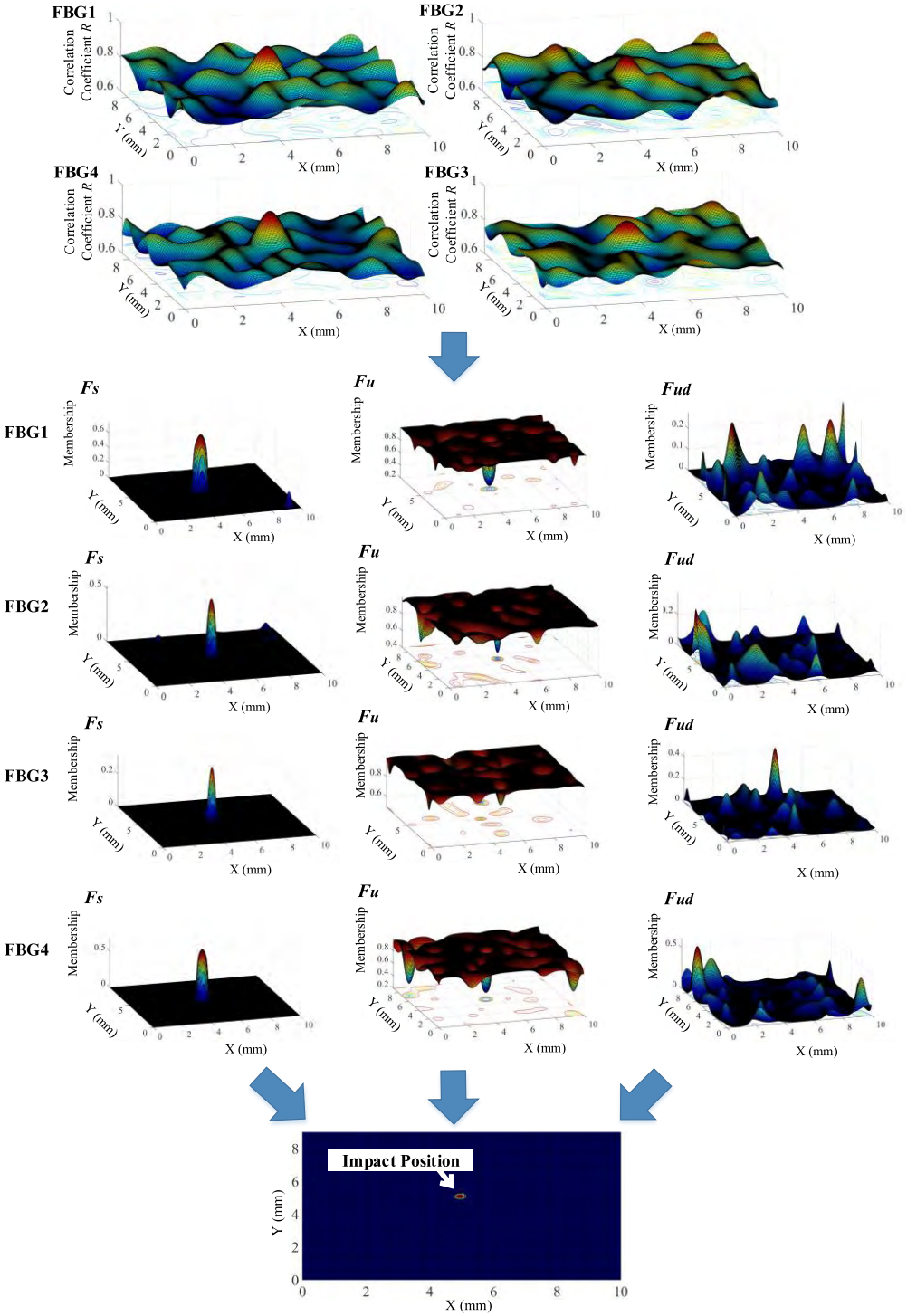

FIGURE 4. The data fusion process by fuzzy evidence theory.

at the points. Four FBG sensors recorded impact signals. The proposed algorithm was run as discussed above.

B. INTERPOLATION COEFFICIENT SETUP

A parametric study was performed to determine the interpolation coefficients p and q. The random impact points from 1 to 20 were used in the study. The average localization errors were calculated with p and q changing from 0 to 4 as shown in Fig. 6.

It can be observed that the average errors are significantly affected by the interpolation coefficients. With p increasing from 0 to 4, the average errors show a downward trend, but

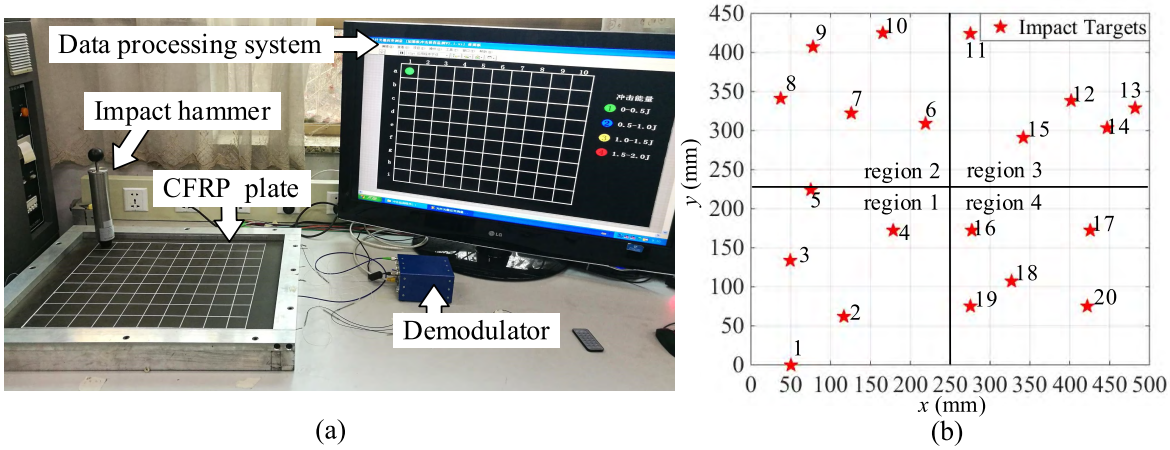

FIGURE 5. Experimental setup and the random impact points. (a) Experimental apparatuses. (b) Impact targets.

TABLE 2. Target coordinates of 20 random impact points.

Local region	Impact targets	x (mm)	y (mm)
1	It_01	50.0	0.0
1	It_02	116.6	61.6
1	It_03	49.0	133.2
1	It_04	178.2	172.4
1	It_05	75.0	224.2
2	It_06	218.8	309.0
2	It_07	125.8	321.7
2	It_08	37.2	341.4
2	It_09	77.5	407.3
2	It_10	165.5	425.4
3	It_11	275.0	424.2
3	It_12	401.7	337.8
3	It_13	482.3	328.7
3	It_14	446.8	303.4
3	It_15	342.1	291.0
4	It_16	277.5	171.7
4	It_17	425.8	171.7
4	It_18	326.9	107.5
4	It_19	275.0	75.0
4	It_20	422.5	75.0

the trend weakens gradually. When p is fixed, the average errors decrease with the increase of q, but the gradient reduces gradually. When p and q are larger than 2, the average errors change little.

The running time of the proposed algorithm with different interpolation coefficients is shown in Fig. 7. It indicates that the time rises with the p and q increasing from 0 to 4. The maximum time is 28.6 s when p and q are both equal to 4. The relationship between the time and q is approximately linear with a specific p. The intervals between adjacent lines are equal. When p and q are 2, the running time is 15.3 s, which is acceptable for the aerospace applications of impact localization algorithms. Hence, p and q are set to be 2 in this paper.

C. DATA FUSION PARAMETER SETUP

Statistical analysis was conducted for training points to determine the data fusion parameters. A total of 5,995 R values

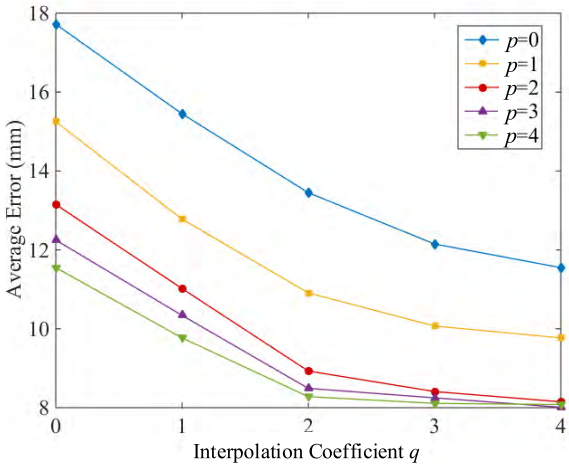

FIGURE 6. The average localization errors for different interpolation coefficients.

were obtained according to the 110 training points. $R_{\max}$, $R_{\min}$, R_{aver}, andR_{sd} were 0.91, 0.63, 0.75, and 0.082, respectively. According to (4), u and σ were 0.75 and 0.082. c_1 and c_2 were 0.91 and 0.63. τ_1 and τ_2 should satisfy $\tau_1 > 75$ and $\tau_2 > 11$. To analyze the influence of τ_1 and τ_2 on the uncertainty of F_s and F_{ud}, τ_1 and τ_2 were both set to be 20, 40, 80, 160, 320, and 640. Basic membership functions of the three fuzzy sets are drawn in Fig. 8.

As shown in Fig. 8, the basic membership functions of the three fuzzy sets overlap each other. F_{ud} is higher than F_u and F_s when the R is relatively low. F_u rises to 1 first, and then decreases to 0 with increasing R. F_{ud} declines to 0 whereas F_s rises to 1 when R is close to 1. The gradients of F_s and F_{ud} are larger with the enhancement of τ_1 and τ_2. Hence, the uncertainty of F_s and F_{ud} decreases. When the τ_1 and τ_2 exceed 160, F_s and F_{ud} are gradually close to the non-fuzzy sets with threshold values 0.91 and 0.63. In this paper, τ_1 and τ_2 are set to be 100 and 35. Fig. 9 exhibits normalized memberships with the determined parameters. F_{ud} is dominant when the R is between 0 and 0.64. F_u is

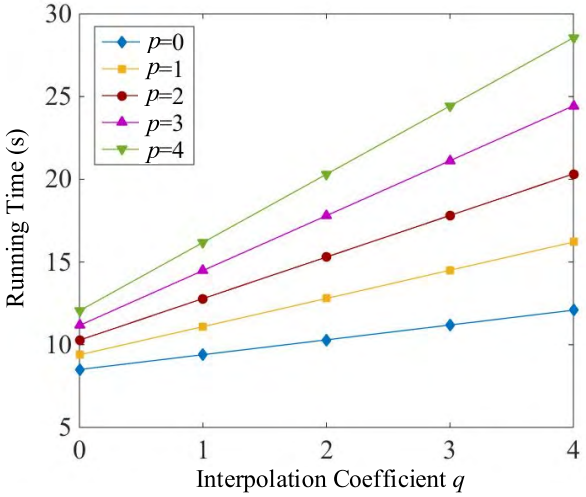

FIGURE 7. The running time with different interpolation coefficients.

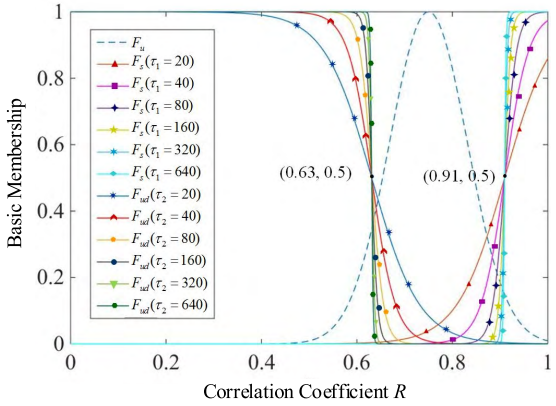

FIGURE 8. Basic membership functions for different τ_1 and τ_2.

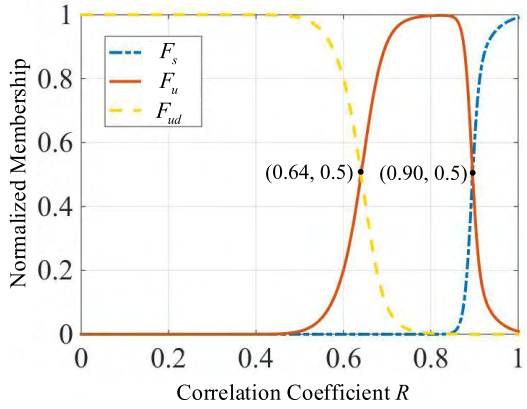

FIGURE 9. Normalized membership with the determined data fusion parameters.

dominant for R between 0.64 and 0.90, and F_s is dominant for R from 0.90 to 1.

IV. RESULTS AND DISCUSSION

A. COMPARISON BETWEEN INTACT SENSOR AND DAMAGED SENSOR

To analyze the influence of sensor damage on the proposed algorithm, the FBG sensor 1 was damaged intentionally, and

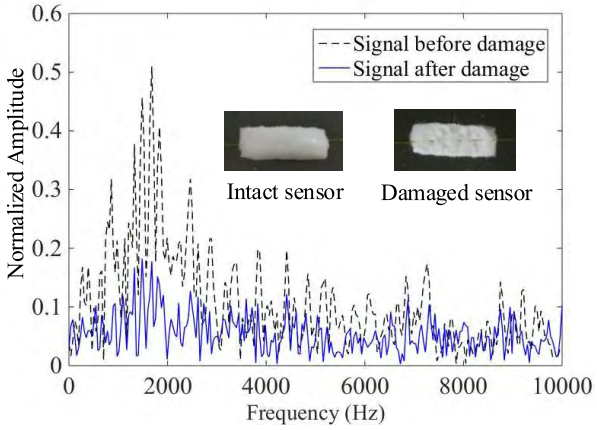

FIGURE 10. Frequency spectrum of the signals recorded by the intact sensor and damaged sensor.

the random impact point 1 was picked as the target point. The signal recorded before the sensor damage was compared to the signal recorded after its damage. The frequency spectrum of the two signals is shown in Fig. 10, and the insets are the intact and damaged sensors.

As seen in Fig. 10, the frequency of both signals is mainly concentrated between 1000 and 3000 Hz. However, for the signal after the sensor damage, the amplitude change is less distinct, and the intensity weakens remarkably. Moreover, the R values before the damage were compared with the R values after the damage for the 110 training points as shown in Fig. 11.

According to Section III. C, the value range of R is divided into 3 intervals by F_s, F_u, and F_{ud}. Before the damage, the maximum R was at training point 2 (50, 0), where it is precisely coincident with the position of a random impact point 1, and the value is higher than 0.9 where F_s is dominant. The R values of the other training points are just between 0.64 and 0.9 in which F_u is dominant. The proposed algorithm classifies the training points properly. After the damage, the R values of all the training points decrease. The position of the maximum R changes to training point 14 (100, 50), which is significantly away from the random impact point 1, and the localization error is 70.7 mm. However, all the R values are lower than 0.64 where F_{ud} is dominant. Hence, the error introduced by sensor damage to the final impact localization is reduced by the proposed algorithm.

B. LOCALIZATION PERFORMANCE WITH DIFFERENT NUMBERS OF DAMAGED SENSORS

To investigate the performance of the proposed algorithm with different numbers of damaged sensors, the localization experiments were conducted with 0 to 3 damaged sensors successively. The relationships between impact localization errors and the number of damaged sensors are shown in Fig. 12.

When there is only one damaged sensor, the average and maximum localization errors are 18.9 mm and 30.2 mm.

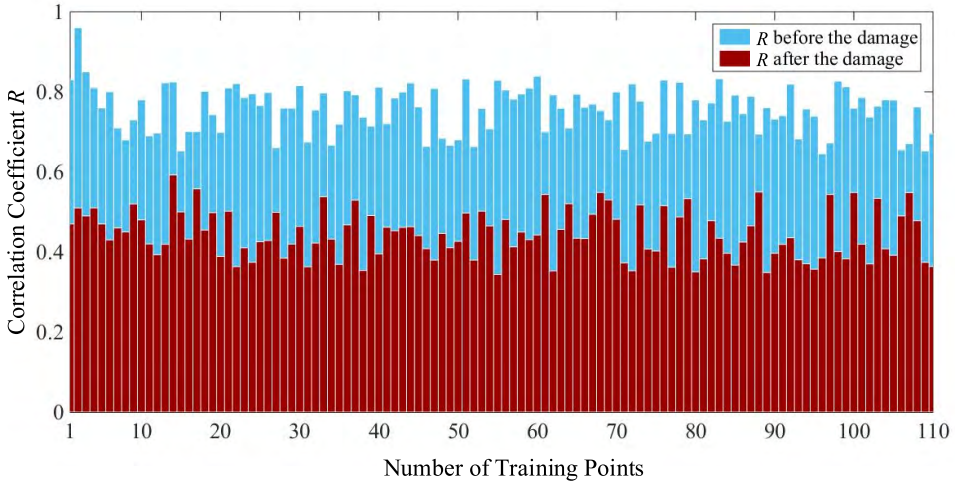

FIGURE 11. The *R* values of the 110 training points before and after the damage.

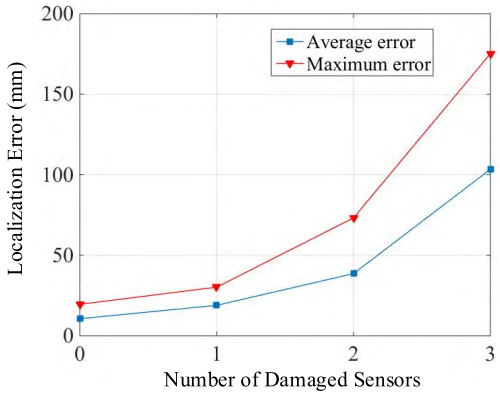

FIGURE 12. The localization errors with different numbers of damaged sensors.

The errors are slightly bigger than those without damaged sensors, but they are less than the 50 mm training spacing. When the number of damaged sensors is 2, the localization errors rise obviously. The average localization error is 38.6 mm. The maximum localization error is 73.2 mm, which is bigger than the training spacing. When 3 sensors are damaged, the average and maximum localization errors rise sharply to 103.4 mm and 175.2 mm, respectively, twice that of the training spacing. In addition, the integrated memberships of the shocked set are 95%, 83%, 48%, and 41% when the number of damaged sensors rises from 0 to 3. The membership indicates the reliability of the impact localization results, which is less than 50% when the number of damaged sensors is more than 1. Therefore, the localization performance of the proposed algorithm is relatively good with 0 or 1 damaged sensors.

C. LOCALIZATION PERFORMANCE IN DIFFERENT MONITORING REGIONS

The localization results of the 20 impact points were obtained when all four sensors were properly functioning. The target points and predicted points are shown in Fig. 13. The average error of the whole monitoring region is 8.6 mm. The maximum localization error is 17.5 mm at point 5, and the minimum localization error is 4.5 mm at point 12. The average errors of the local region 1 to local region 4 were also calculated according to the localization results of these regions, which are 8.6 mm, 7.4 mm, 8.0 mm, and 10.5 mm. It can be concluded that the average localization errors have a small difference from local region 1 to local region 4, which is due to the symmetry of the spatial arrangement of the impact monitoring region.

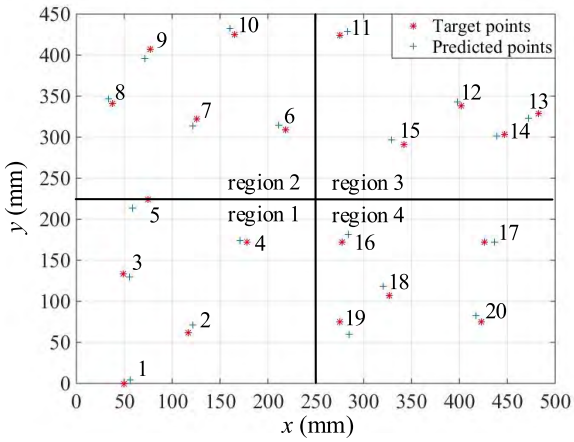

FIGURE 13. The target points and predicted points obtained by 4 properly functioning sensors.

The proposed algorithm was also carried out when FBG sensor 1 was damaged. The localization results are shown in Fig. 14. The localization errors have increased compared with the results of properly functioning sensors, and the distribution of errors along the monitoring regions has also changed. The average error of the whole monitoring region is 18.9 mm. The maximum and minimum localization

TABLE 3. Comparison results of the localization performance.

Algorithm	Running time (s)	Properly functioning condition		Damaged condition	
		Average error (mm)	Maximum error (mm)	Average error (mm)	Maximum error (mm)
Neural Network	13.7	9.8	24.6	58.7	88.9
Wave Propagation	6.9	11.4	26.5	75.6	102.3
Traditional Reference Database	8.5	19.8	28.0	46.2	85.5
Current Work	15.3	8.6	19.5	18.9	30.2

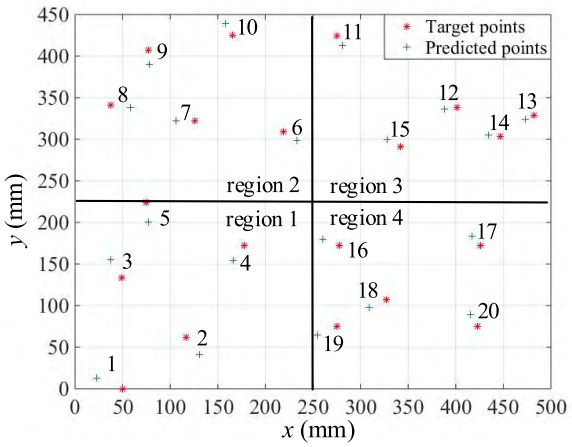

FIGURE 14. The target points and predicted points obtained under the damage of sensor 1.

errors are 30.2 mm at point 1 and 10.4 mm at point 13, respectively. Among the 20 random impact points, most of the relatively large localization errors appear near the position of sensor 1. The average error of local region 1 is 25.2 mm, and it is significantly larger than the errors of the other 3 local regions, which are 18.4 mm for region 2, 13.3 mm for region 3 and 18.8 mm for region 4. The localization accuracy of the proposed algorithm is relatively low when the random impact points are near the position of the damaged sensor. In fact, the proposed algorithm reduces the decision-making power of the damaged sensor according to the fuzzy evidence theory. Therefore, the final localization results mainly depend on the other properly functioning sensors. The localization accuracy is enhanced when the random impact points are close to these properly functioning sensors. The experimental results are in accordance with the theoretical analysis.

D. THE LOCALIZATION PERFORMANCE COMPARISON

To check the localization performance of the proposed algorithm, the localization results were compared with the results of the neural network algorithm [13], the wave propagation algorithm [16] and the traditional reference database algorithm [20]. In this paper, the comparison of experiments was conducted with the same conditions as described in Section III. A. The 110 training points served as training set, and the 20 random impact points served as validation set. The experiments were carried out under the normal condition with 4 properly functioning sensors and the damaged condition with 1 or more damaged sensors. The running time of these algorithms was recorded, and the average and maximum localization errors were calculated as shown in Table 3.

The running time ranges from 6.9 s to 15.3 s, and the time of the proposed algorithm is higher than that of other algorithms. Compared with the traditional reference database algorithm, the proposed algorithm mainly consumes time in the interpolation and data fusion processes. For the normal condition, the average localization error of the proposed algorithm is 8.6 mm, smallest among all the algorithms. The neural network algorithm is in the second place with 9.8 mm, and the traditional reference database algorithm is in last place with 19.8 mm. The maximum localization error of the proposed algorithm is 19.5 mm, significantly better than the errors of other algorithms, which range from 24.6 mm to 28.0 mm. The proposed algorithm obtains the highest accuracy among all the algorithms without damaged sensors. In the case of sensor damage, the maximum localization errors of all the algorithms are more than the space of 50 mm between adjacent training points if the number of damaged sensors is more than one. However, when there is one damaged sensor, the average error and maximum error of the proposed algorithm are 18.9 mm and 30.2 mm, respectively. The traditional reference database algorithm is in the second place. Compared with the results of the traditional reference database algorithm, the average error and maximum error are reduced by 59.1 % and 64.7 %, respectively. The localization accuracy of the proposed algorithm is obviously superior to the other algorithms.

V. CONCLUSION

This study suggests a low-velocity impact localization algorithm based on interpolation reference database and fuzzy evidence theory to realize accurate localizations on composites under sensor damage. A basic reference database is first established. More correlation coefficients can be obtained by the double cubic polynomial interpolation. Then, the fuzzy evidence theory is used to evaluate the reliability of the FBG sensors. The influence of damaged sensors on the localization results is reduced.

The experiment results show the localization performance of the proposed algorithm has been significantly improved. The average error and maximum error are 8.6 mm and 19.5 mm, respectively, when all four sensors are running

properly. When one of the sensors is damaged, the average error is 18.9 mm, 40.9 % of the traditional reference database algorithm, and the maximum error is 30.2 mm, 35.3 % of the traditional reference database algorithm. The localization results are much smaller than the results of the other algorithms according to the comparison. Therefore, the proposed algorithm has a strong ability to address the signal from the damaged sensor.

Since the proposed algorithm can realize the impact localization under sensor damage, more reliable and accurate information can be provided to pilots and maintenance engineers for inspection, which is of great significance to the aerospace applications of composites.

REFERENCES

[1] M. Hong, Z. Mao, M. D. Todd, and Z. Su, "Uncertainty quantification for acoustic nonlinearity parameter in Lamb wave-based prediction of barely visible impact damage in composites," *Mech. Syst. Signal Process.*, vol. 82, pp. 448–460, Jan. 2017.

[2] M. Jiang, S. Lu, Q. Sui, H. Dong, Y. Sai, and L. Jia, "Low velocity impact localization on CFRP based on FBG sensors and ELM algorithm," *IEEE Sensors J.*, vol. 15, no. 8, pp. 4451–4456, Aug. 2015.

[3] P. Shrestha, Y. Park, and C.-G. Kim, "Low velocity impact localization on composite wing structure using error outlier based algorithm and FBG sensors," *Compos. B, Eng.*, vol. 116, pp. 298–312, May 2017.

[4] D. Montalvão, A. M. R. Ribeiro, and J. Duarte-Silva, "A method for the localization of damage in a CFRP plate using damping," *Mech. Syst. Signal Process.*, vol. 23, no. 6, pp. 1846–1854, 2009.

[5] M. Chandrashekhar and R. Ganguli, "Damage assessment of composite plate structures with material and measurement uncertainty," *Mech. Syst. Signal Process.*, vol. 75, pp. 75–93, Jun. 2016.

[6] A. Ryosi, M. Valentino, G. Peluso, and G. Pepe, "Analysis of low-velocity impact damage in reinforced carbon fiber composites by HTS-SQUID magnetometers," *IEEE Trans. Appl. Supercond.*, vol. 11, no. 1, pp. 1172–1175, Mar. 2001.

[7] H. Liu, S. Liu, Z. Liu, N. Mrad, and H. Dong, "Prognostics of damage growth in composite materials using machine learning techniques," in *Proc. IEEE Int. Conf. Ind. Technol.*, Mar. 2017, pp. 1042–1047.

[8] L. Qiu, S. Yuan, P. Liu, and W. Qian, "Design of an all-digital impact monitoring system for large-scale composite structures," *IEEE Trans. Instrum. Meas.*, vol. 62, no. 7, pp. 1990–2002, Jul. 2013.

[9] S. Yuan, Y. Ren, L. Qiu, and H. Mei, "A multi-response-based wireless impact monitoring network for aircraft composite structures," *IEEE Trans. Ind. Electron.*, vol. 63, no. 12, pp. 7712–7722, Dec. 2016.

[10] E. Z. Moore, J. M. Nichols, and K. D. Murphy, "Model-based SHM: Demonstration of identification of a crack in a thin plate using free vibration data," *Mech. s Signal Process.*, vol. 29, pp. 284–295, May 2012.

[11] Y. Mei, X. Yao, S. Hao, and W. Wenjuan, "An under sampled impact location method based on FBG sensor," in *Proc. IEEE Int. Conf. Aircraft Utility Syst. (AUS)*, Beijing, China, Oct. 2016, pp. 130–134.

[12] L. Morse, Z. S. Khodaei, and M. H. Aliabadi, "Reliability based impact localization in composite panels using Bayesian updating and the Kalman filter," *Mech. Syst. Signal Process.*, vol. 99, pp. 107–128, Jan. 2018.

[13] B.-W. Jang, Y.-G. Lee, J.-H. Kim, Y.-Y. Kim, and C.-G. Kim, "Real-time impact identification algorithm for composite structures using fiber Bragg grating sensors," *Structural Control Health Monit.*, vol. 19, no. 7, pp. 580–591, 2012.

[14] C. Y. Park, J. H. Kim, S.-M. Jun, and C.-G. Kim, "Localizations and force reconstruction of low-velocity impact in a composite panel using optical fiber sensors," *Adv. Composite Mater.*, vol. 21, nos. 5–6, pp. 357–369, 2012.

[15] Y. Ren, L. Qiu, S. Yuan, and Z. Su, "A diagnostic imaging approach for online characterization of multi-impact in aircraft composite structures based on a scanning spatial-wavenumber filter of guided wave," *Mech. Syst. Signal Process.*, vol. 90, pp. 44–63, Jun. 2017.

[16] J. Frieden, J. Cugnoni, J. Botsis, T. Gmür, "Low energy impact damage monitoring of composites using dynamic strain signals from FBG sensors—Part I: Impact detection and localization," *Composite Struct.*, vol. 94, no. 2, pp. 438–445, 2012.

[17] Y. Sai, M. Jiang, Q. Sui, S. Lu, and L. Jia, "FBG sensor array-based-low speed impact localization system on composite plate," *J. Mod. Opt.*, vol. 63, no. 5, pp. 462–467, 2016.

[18] B.-W. Jang and C.-G. Kim, "Impact localization on a composite stiffened panel using reference signals with efficient training process," *Compos. B, Eng.*, vol. 94, pp. 271–285, Jun. 2016.

[19] B.-W. Jang, Y.-G. Lee, C.-G. Kim, and C.-Y. Park, "Impact source localization for composite structures under external dynamic loading condition," *Adv. Composite Mater.*, vol. 24, no. 4, pp. 359–374, 2015.

[20] P. Shrestha, J.-H. Kim, Y. Park, and C.-G. Kim, "Impact localization on composite wing using 1D array FBG sensor and RMS/correlation based reference database algorithm," *Composite Struct.*, vol. 125, pp. 159–169, Jul. 2015.

[21] P. Shrestha, J.-H. Kim, Y. Park, and C.-G. Kim, "Impact localization on composite structure using FBG sensors and novel impact localization technique based on error outliers," *Composite Struct.*, vol. 142, pp. 263–271, May 2016.

[22] P. Dandan, S. Qingmei, Z. Guiqing, W. Ming, and X. Hongdong, "Impact localization based on FBG sensing system with broadband light source," in *Proc. IEEE Inf. Technol., Netw., Electron. Automat. Control Conf.*, Chongqing, China, May 2016, pp. 986–989.

[23] T. Fu, Y. Liu, K.-T. Lau, and J. Leng, "Impact source identification in a carbon fiber reinforced polymer plate by using embedded fiber optic acoustic emission sensors," *Compos. B, Eng.*, vol. 66, pp. 420–429, Nov. 2014.

[24] E. Kirkby, R. de Oliveira, V. Michaud, J. A. Månson, "Impact localisation with FBG for a self-healing carbon fibre composite structure," *Composite Struct.*, vol. 94, no. 1, pp. 8–14, 2011.

[25] A. Rezayat *et al.*, "Reconstruction of impacts on a composite plate using fiber Bragg gratings (FBG) and inverse methods," *Composite Struct.*, vol. 149, pp. 1–10, Aug. 2016.

[26] J.-H. Kim, Y.-Y. Kim, Y. Park, and C.-G. Kim, "Low-velocity impact localization in a stiffened composite panel using a normalized cross-correlation method," *Smart Mater. Struct.*, vol. 24, no. 4, p. 045036, 2015.

[27] Q. Jiang, X. Jin, S.-J. Lee, and S. Yao, "A novel multi-focus image fusion method based on stationary wavelet transform and local features of fuzzy sets," *IEEE Access*, vol. 5, pp. 20286–20302, 2017.

[28] Z. Zhang, Z. Hao, S. Zeadally, J. Zhang, B. Han, and H.-C. Chao, "Multiple attributes decision fusion for wireless sensor networks based on intuitionistic fuzzy set," *IEEE Access*, vol. 5, pp. 12798–12809, 2017.

[29] Y. Zhang, Y. Liu, Z. Zhang, H.-C. Chao, J. Zhang, and Q. Liu, "A weighted evidence combination approach for target identification in wireless sensor networks," *IEEE Access*, vol. 5, pp. 21585–21596, 2017.

[30] H. Xu and Y. Deng, "Dependent evidence combination based on Shearman coefficient and Pearson coefficient," *IEEE Access*, vol. 6, pp. 11634–11640, 2018.

[31] P. Stpiczynski and J. Potiopa, "Piecewise cubic interpolation on distributed memory parallel computers and clusters of workstations," in *Proc. Int. Symp. Parallel Comput. Electr. Eng. (PAR ELEC)*, Bialystok, Poland, Sep. 2006, pp. 284–289.

[32] F. J. Aparicio-Navarro, K. G. Kyriakopoulos, Y. Gong, D. J. Parish, and J. A. Chambers, "Using pattern-of-life as contextual information for anomaly-based intrusion detection systems," *IEEE Access*, vol. 5, pp. 22177–22193, 2017.

HONGYANG LI was born in Chengdu, China, in 1990. He received the B.S. degree in measurement and control technology from the Hefei University of Technology, Hefei, China, in 2010. He is currently pursuing the Ph.D. degree in instrument science and technology from Beihang University, Beijing, China. His current research interests include structural health monitoring, data fusion, and decision making in fiber sensor networks.

ZHONGYU WANG was born in Luoyang, China, in 1963. He received the B.S. and M.S. degrees in precision engineering from the Hefei University of Technology, Hefei, China, in 1985 and 1988, respectively, and the Ph.D. degree in mechanical engineering from the Huazhong University of Science and Technology, Wuhan, China, in 1996. He is currently a Professor with the School of Instrumentation Science and Opto-electronics Engineering, Beihang University, Beijing, China. He is on the Editorial Board of the *Journal of Grey System*.

JEFFREY YI-LIN FORREST was born in Fuzhou, Fujian, China, in 1959. He received the B.S. degree in pure mathematics and the M.S. degree in general topology from Northwest University, Xi'an, in 1982 and 1984, respectively, and the Ph.D. degree from Auburn University, Alabama, in 1988, under the supervision of B. Fitzpatrick. Since 2002, he has been a Professor in mathematics with Slippery Rock University, Slippery Rock, PA, USA.

WENSONG JIANG was born in Anqing, China, in 1988. He received the B.S. and M.S. degrees in mechanical engineering from China Jiliang University, Hangzhou, China, in 2013. He is currently pursuing the Ph.D. degree in mechanical engineering from Beihang University, Beijing, China. He has published seven articles and patented 19 inventions.